Biofilm 4 (2022) 100078

Contents lists available at ScienceDirect

Biofilm

journal homepage: www.sciencedirect.com/journal/biofilm

Mobility of extracellular DNA within gonococcal colonies

Niklas Bender [a], Marc Hennes [a], Berenike Maier [a,b,*]

[a] Institute for Biological Physics, University of Cologne, Zülpicherstr. 47a, 50647, Köln, Germany
[b] Center for Molecular Medicine Cologne, Germany

A B S T R A C T

Transformation enables bacteria to acquire genetic information from extracellular DNA (eDNA). Close proximity between bacteria in colonies and biofilms may inhibit escape of eDNA from the colony but it also hinders its diffusion between donor and recipient. In this study, we investigate the mobility of DNA within colonies formed by *Neisseria gonorrhoeae*, and relate it to transformation efficiency. We characterize the penetration dynamics of fluorescent DNA into the colony at a time scale of hours and find that 300 bp fragments diffuse through the colony without hindrance. For DNA length exceeding 3 kbp, a concentration gradient between the edge and the center of the colony develops, indicating hindered diffusion. Accumulation of DNA within the colony increases with increasing DNA length. The presence of the gonococcal DNA uptake sequence (DUS), which mediates specific binding to type 4 pili (T4P) and uptake into the cell, steepens the radial concentration gradient within the colony, suggesting that the DUS reduces DNA mobility. In particular, DNA of *N. gonorrhoeae* containing multiple DUS is trapped at the periphery. Under conditions, where DUS containing DNA fragments readily enter the colony center, we investigate the efficiency of transformation. We show that despite rapid diffusion of DNA, the transformation is limited to the edge of young colonies. We conclude that DNA mobility depends on DNA length and specific binding mediated by the DUS, resulting in restricted mobility of gonococcal DNA. Yet gonococcal colonies accumulate DNA, and may therefore act as a reservoir for eDNA.

1. Introduction

Biofilms have often been labeled “bioreactors” and “hot spots” for horizontal gene transfer [1–3]. In particular, the contact-dependent mechanisms for gene transfer, conjugation, and nanotube formation depend on close proximity between donor and recipient of transferred genes [1,3,4]. Yet, different bacterial strains and species segregate [5] and inhabit different regions of a biofilm [6–8], which minimizes the contact zones where genetic exchange can occur. Transformation can occur even if donor and recipient are at a distance. By means of diffusion, extracellular DNA (eDNA) may cover large distances within a biofilm and enable the exchange of genetic material between species residing at different biofilm locations. However, it is currently unknown how mobile eDNA is within biofilms. Diffusivity of small molecules and inert polymers are reduced in bacterial biofilms [9–11]. In this study, we investigate the mobility of eDNA within early biofilms.

Transformation is one mechanism of horizontal gene transfer. During transformation, eDNA binds to the surface of a competent cell and is, subsequently, imported into the cytoplasm [12]. The transformation mechanism of the human pathogen *Neisseria gonorrhoeae* is well characterized. The type IV pilus (T4P) [13] is responsible for initial binding of DNA to the cell surface [14,15]. The binding probability is modulated by the DNA uptake sequence (DUS) [16], a specific- 10 bp to 12 bp sequence that interacts with the minor pilin, ComP [17–19]. These sequences represent up to 1% of the entire genome and are 1000-fold more common than statistically expected [18]. This ensures that the probability that genus specific-DNA is taken up is several orders of magnitude higher compared to the uptake probability of DNA derived from other species [14,16,17,20]. Bound eDNA is taken up into the periplasm by a translocation ratchet mechanism driven by the DNA-binding chaperone ComE [21,22]. Once imported into the cytoplasm, the newly acquired DNA can be integrated into the chromosome by homologous recombination.

N. gonorrhoeae is the causative agent of gonorrhea, the second most common sexually transmitted disease. There is evidence that gonococcal biofilms form in vivo and they are thought to be associated to long-term asymptomatic carriage in women [23,24]. eDNA is a component of the biofilm matrix [25] and stabilizes early biofilms [26,27]. Gonococcal T4P are dynamic cell appendages [28,29] that mediate surface motility [28] and assembly into (micro)colonies consisting of several thousands of bacteria both -on inert surfaces and on a layer of host cells [30,31]. In vitro, colonies formed by *N. gonorrhoeae* and the closely related *Neisseria meningitidis* have developed into a model system that allows studying the mechanical properties of colonies systematically. In particular, assembly of colonies, their fluidity, and susceptibility to antibiotic treatment are determined by T4P and their motor dynamics [5,32–34,35]. Colony

* Corresponding author. Institute for Biological Physics, University of Cologne, Zülpicherstr. 47a, 50647, Köln, Germany.
E-mail address: berenike.maier@uni-koeln.de (B. Maier).

https://doi.org/10.1016/j.bioflm.2022.100078
Received 21 January 2022; Received in revised form 10 May 2022; Accepted 10 May 2022
Available online 20 May 2022

formation is reversible in small colonies; for example upon oxygen depletion, colonies disassemble [27]. In larger colonies with more than ~ 1000 bacteria, a stable kernel forms that does not disassemble at low oxygen concentrations. In these colonies, a gradient of growth rates develops within ~ 2 h, whereby bacteria residing at the center stop growing [36]. Furthermore, there is evidence that gene expression becomes heterogeneous [37]. We propose that the transition from reversible to irreversible aggregation and heterogeneity of growth rates and gene expression signify the onset of biofilm formation. Taken together, gonococcal colonies comprising several thousand cells are a well-controlled and tunable model for early gonococcal biofilms.

In a previous study, we investigated the efficiency of transformation in gonococcal biofilms [38]. We found that transformation occurred in early biofilms at a higher rate compared to planktonic cells. The low fraction of transformation of $<10^{-4}$ prohibited direct imaging of transformation under non-selective conditions. Transformation was studied between two strains that were well mixed within biofilms because they had the same surface properties. However, when we address gene transfer between different species, we expect that they segregate as a consequence of different surface properties [5]. Therefore, the mobility of eDNA is a critical factor determining the probability of gene transfer within biofilms.

In this study, we investigate the spatio-temporal dynamics of eDNA penetration into gonococcal colonies. We focus on the length dependence of DNA mobility and DNA accumulation and on the role of specific binding of DNA to T4P via their DUS. We show that DNA fragments with lengths corresponding to a single gene or a single operon rapidly penetrate the biofilm. Retention of DNA increases with DNA length. It was conceivable that the DUS either enhances or reduces DNA mobility. Specific binding to the T4P might reduce the mobility, yet active T4P dynamics could also help shuffling DNA through the colony. We find that DNA from a different species that does not contain DUS penetrates the colonies much more efficiently than gonococcal DNA containing many DUS. Finally, we use the results gained about DNA mobility to probe for transformation under conditions, where DNA fragments penetrate the entire colony on the time scale of 1 h. We find that transformation is localized to the edge of the colony, suggesting that bacteria residing at the center of the colony are impaired for transformation.

2. Results

2.1. Spatio-temporal dynamics of DUS-free DNA within colonies

First, we characterized the mobility of unspecific DNA fragments within gonococcal colonies. With this assay, we characterize the localization of eDNA. DNA that contains no DNA uptake sequence (DUS) does not bind specifically to T4P [18] and no DNA uptake is detectable using fluorescently labeled DNA [22]. DNA was labeled with the fluorescent dye Cy3 (Cy3-DNA). Gonococci actively assemble into colonies comprising thousands of cells by means of T4P-T4P interaction [32,34,36]. In this study, colonies were formed in liquid media for 30 min prior to inoculating them to microscopy slides. At the positively charged glass surface, colonies are motile and fuse to form larger colonies. After 30 min at the surface, the colonies tend to become immotile and colony growth is determined by cellular proliferation. At this time, fluorescently labeled DNA was added. We imaged colonies for 2 h and determined the radial fluorescence intensity profiles as described in the Methods section.

We found that 300 bp Cy3-DNA fragments caused a small increase in fluorescence intensity relative to the background (Fig. 1A, D), indicating that the fragments penetrate the colony. If the DNA fragments would not

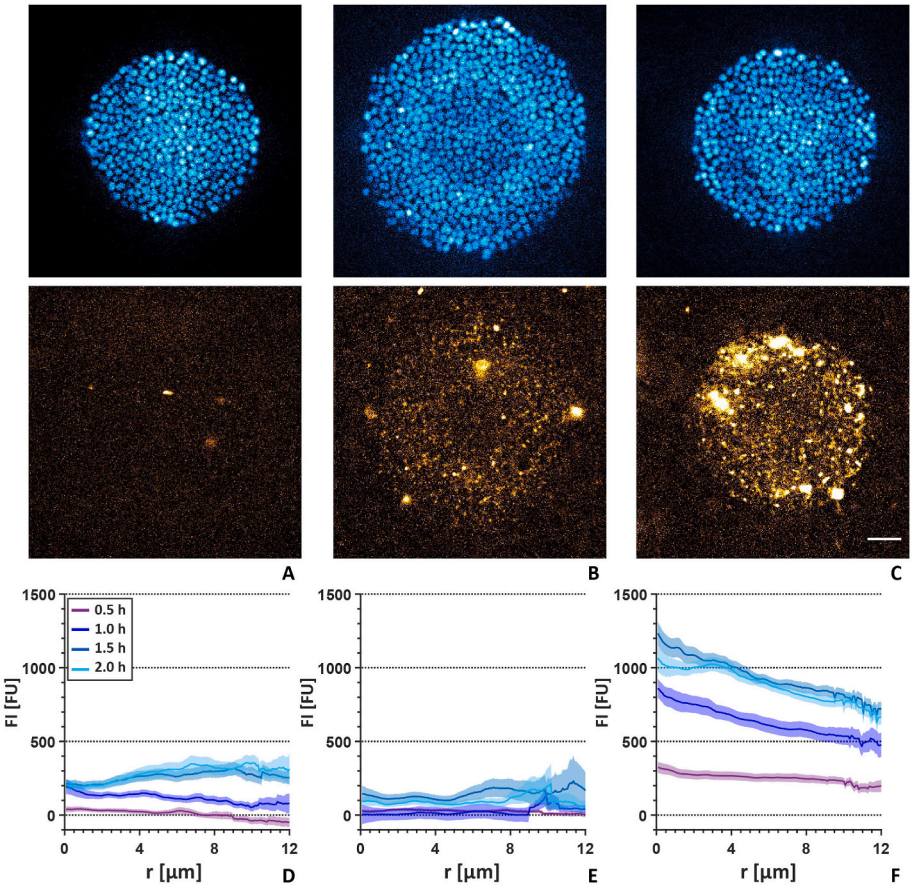

Fig. 1. Spatio-temporal dynamics of DNA without DUS within gonococcal colonies. Typical confocal slices of colonies formed by strain wt* (NG194) imaged 2 h after addition of Cy3-DNA. (A–C) Upper image: sfGFP signal denoting cell positions. Lower image: Cy3-DNA. A) 300 bp fragments, B) 3 kb fragments, C) DNA isolated from *E. coli*. (D–E) Mean radial fluorescence intensity (FI) in arbitrary fluorescence units (FU) per μm^3 of Cy3-DNA as a function of the distance (r) to the colony contour. D) 300 bp fragments, E) 3 kb fragments, F) DNA isolated from *E. coli*. Shaded areas represent standard errors of 26 – 38 colonies. Scale bar: 5 µm.

penetrate the colony, the fluorescence intensity within the colony would be lower compared to the background. For 3 kbp fragments, the increase in fluorescence intensity within the colony was more pronounced (Fig. 1B). It increased as a function of time and became saturated after 1.5 h. Initially, the radial intensity profile showed a decay towards the center of the colony, suggesting that diffusion of DNA into the colony was hindered. After 1 h, however, the profile flattened, which indicates homogeneous distribution of DNA across the entire colony. Furthermore, we investigated the mobility of DNA from a genetically distinct species, *Escherichia coli*. The total DNA contains fragments of genomic DNA obtained after purification as described in the Methods. The dominating fragment size exceeds 10 kbp, but shorter fragments are present as well (Fig. S6). The *E. coli* genome carries 12 truncated 10 bp DUS sequences, but no full-length DUS. Interestingly, the total fluorescence signal was stronger compared to the intensity created by 3 kbp Cy3-DNA. We find that the intensity increases continuously during the initial 1-1.5 h and saturates thereafter (Fig. 1C, F). The profile shows a strong decline from the colony edge towards inner layers of the colony, indicating that diffusion of DNA from a different species is hindered. Still, a fraction of DNA molecules readily penetrates the colony and reaches the colony center.

Unexpectedly, few cells within the colony exhibit an exceptionally strong fluorescence signal. By adjusting the contrast (Fig. S1), we find that the Cy3-DNA signal localized to the cellular periphery in these cells. The occurrence of bright cells was independent of DNA length and of the presence of a DUS. Using SytoX staining, we assessed whether these cells with a particular strong fluorescence signal were dead, in which case Cy3-DNA could permeate the ruptured, outer cell envelope. However, we found no correlation between the Cy3-DNA signal and the one of SytoX, indicating that the bright signal was not caused by dead cells.

We conclude that DNA containing no or only few DUS penetrates gonococcal colonies readily. However, for long DNA fragments, we find signatures of hindered diffusion. With increasing fragment length, colonies retain an increasing amount of DNA.

2.2. The DNA uptake sequence (DUS) affects the spatio-temporal dynamics of DNA

The DUS enhances the probability of DNA binding and uptake by several orders of magnitude [14]. It was, thus, conceivable, that the DUS affects the penetration of DNA into gonococcal colonies. We repeated the experiment described in the previous paragraph using Cy3-DNA fragments that contained a single or multiple DUS (Fig. 2). With this assay, we detect both eDNA and DNA taken up into the periplasm.

When treated with 300 bp fragments, colonies showed a spatially homogeneous fluorescence signal which increased as a function of time, indicating that short fragments readily penetrated the cell aggregates (Fig. 2A, D). The fluorescence intensities were considerably higher compared to colonies treated with DNA lacking any DUS. When treated with 3 kb fragments, the intensity profiles showed a slope at early time points indicative of hindered penetration (Fig. 2B, E). After 1 h, the intensity profiles became flat, indicating homogeneous distribution. The fluorescence intensities were higher compared to intensities in colonies treated with fragments that contained no DUS.

Treatment with DNA isolated from *N. gonorrhoeae* (gonococcal DNA) generated strikingly different intensity profiles. At the periphery of the colony, the Cy3-DNA fluorescence increased continuously and saturated after 1.5 h (Fig. 2C, F). With increasing penetration depth into the colony (r) the intensity decreased exponentially. Even after 2 h, the fluorescence intensity at the center of the colony did not exceed background levels, indicating that diffusion of genomic DNA is inhibited in the colonies. We note that the negative values of fluorescence intensity at the center of the colony indicate that there is less Cy3-DNA at the center of the colony than within the solution outside of the colony. The

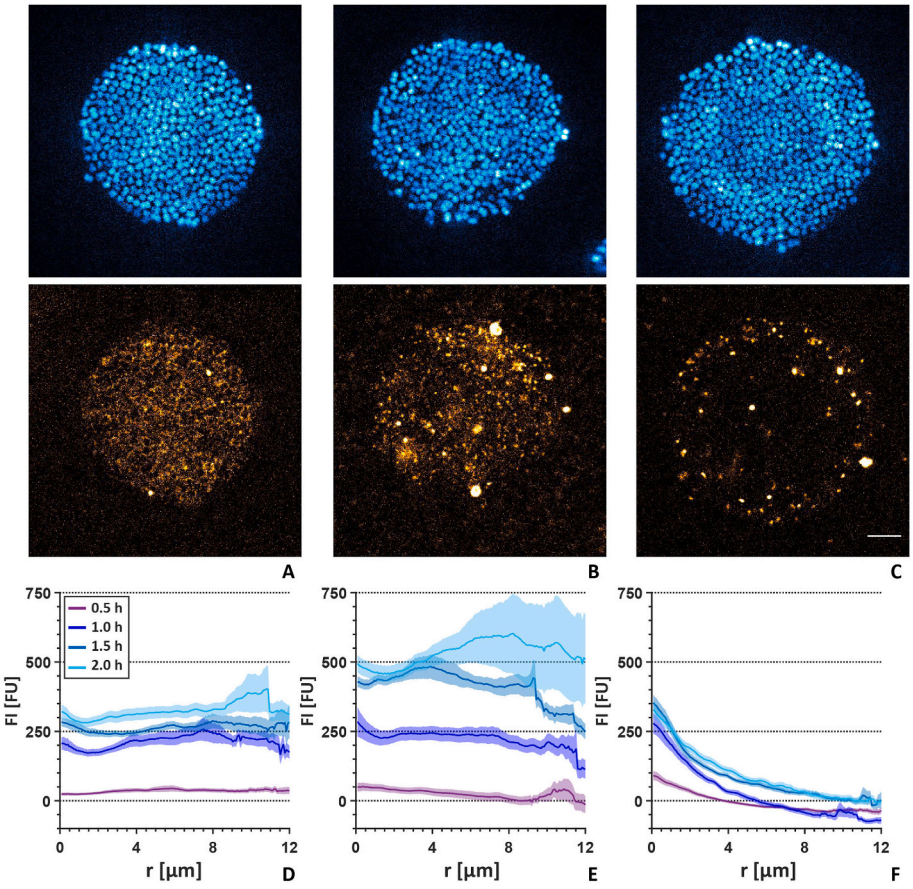

Fig. 2. Spatio-temporal dynamics of DNA containing DUS within gonococcal colonies. Exemplary confocal slices of colonies formed by strain wt* (NG194) imaged 2 h after addition of Cy3-DNA. (A–C) Upper image: sfGFP signal denoting cell positions. Lower image: Cy3-DNA. A) 300 bp fragments, B) 3 kb fragments, C) DNA isolated from *N. gonorrhoeae*. (D–E) Mean radial fluorescence intensity (FI) in arbitrary fluorescence units (FU) per µm^3 of Cy3-DNA as a function of the distance (r) to the colony contour. D) 300 bp fragments, E) 3 kb fragments, F) DNA isolated from *N. gonorrhoeae*. Shaded areas represent standard errors of 30 – 39 colonies. Scale bar: 5 µm.

background subtraction procedure is explained in the Methods. Preparations of gonococcal DNA contain chromosomal DNA and plasmid DNA including the cryptic plasmid (Figs. S6 and 37). To find out how the plasmid DNA behaves within colonies, we enriched the genomic DNA preparation for plasmid DNA, labeled it with Cy3, and characterized its spatial distribution within the colony. We find that less DNA accumulates at the periphery and more DNA is retained within the center of the colony when compared to the mixture of chromosomal and plasmid DNA (Fig. S2). This indicates that plasmid DNA is overrepresented at the center of the colony.

N. gonorrhoeae generate the nuclease Nuc which likely resides within the periplasm and the exterior of the cells [20,25,39]. We asked whether deletion of *nuc* affected the Cy3-DNA intensity profiles within colonies. To this end, we repeated the experiment with colonies formed by a *Δnuc* strain (Fig. 3, Fig. S3). We find that gonoccal DNA is more abundant in colonies formed by *Δnuc* compared to *wt** colonies (Fig. 3), indicating that Nuc degrades gonococcal DNA residing within colonies. By contrast, deletion of *nuc* showed only minor effects on the intensity profiles of 300 bp and 3 kb DNA fragments (Fig. S3).

We addressed the question how DNA isolated from a closely related species spreads through the colony. *Neisseria cinerea* has the same consensus DNA uptake sequence as *N. gonorrhoeae* [17], yet it has a different methylation pattern [40,41] (http://tools.neb.com/genomes/index.php?page=N). In particular, *N. gonorrhoeae* MS11 encodes 16 methyltransferases whereas *N. cinerea* encodes only 3 predicted methyltransferases [40]. We generated Cy3-labeled DNA from *N. cinerea* and determined the radial distribution of fluorescence intensities (Fig. S4A). Qualitatively, its spatial pattern is similar to the pattern formed by gonococcal DNA. The total fluorescence intensities are lower, indicating that less *N. cinerea* DNA than *N. gonorrhoeae* is retained within the colonies. Methylation protects gonococcal DNA from degradation by Nuc [25]. To find out whether the difference is caused by Nuc-dependent degradation, we repeated the experiment with colonies formed by the gonococcal *Δnuc* strain. At early times, deletion of *nuc* showed little effect on the amount of *N. cinerea* DNA retained within the colony (Fig. S4). However, after 2 h, the amount of *N. cinerea* DNA was considerably higher in *Δnuc* colonies compared to wt* colonies, indicating that Nuc affects DNA retention.

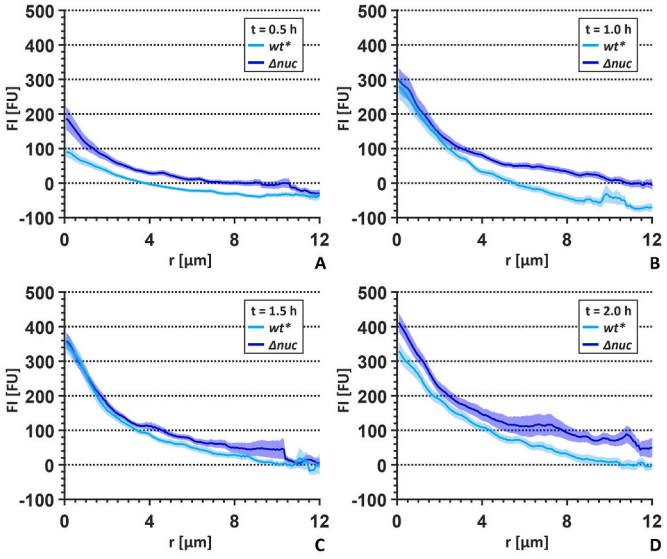

Fig. 3. The nuclease Nuc reduces gonococcal DNA within colonies. Mean radial fluorescence intensities (FI) in arbitrary fluorescence units (FU) per μm^3 of Cy3-labeled gonococcal DNA as a function of the distance (r) to the colony contour immediately after addition to the medium (A), and after 0.5 h (B), 1 h (C) and 2 h (D), for colonies formed by wildtype (*wt**, NG194) and *nuc*-deletion (*Δnuc*, NG235) strains. Shaded areas represent standard errors of 33 – 40 colonies.

In summary, we find that the presence of DUS strongly affects the spatio-temporal dynamics of DNA in gonococcal colonies. Penetration of short DNA is efficient and eventually leads to uniform accumulation of DNA across the colony, while DNA derived from *N. gonorrhoeae* and *N. cinerea* penetrates colonies poorly. The thermonuclease Nuc reduces the density of gonococcal DNA.

2.3. Focus-formation by the periplasmic DNA-binding protein ComE

Next, we set out to uncover the dynamics of DNA uptake within gonococcal biofilms by investigating ComE foci formation in colonies formed by *N. gonorrhoeae*. To this end, we created a strain expressing one of the four gene copies of *comE* as a fusion to *mcherry* (*comE-mcherry*). In isolated gonococci, ComE-mCherry was shown to be homogeneously distributed in the absence of eDNA [22]. Within minutes after the addition of eDNA, ComE-mCherry formed foci at the site of DNA uptake. Therefore, we intended to use focus formation to identify the locations of DNA uptake within colonies. To this end, the distribution of ComE-mCherry was imaged within gonococcal colonies and the local density of ComE-mCherry foci was determined as described in the Methods and Fig. S5.

We compared ComE-mCherry focus formation under three different conditions; without treatment, after adding gonococci DNA, and after adding DNase. After 1 h, we found that foci formed in the absence of treatment and their distribution was homogeneous (Fig. 4A, D). Addition of gonococcal DNA hat little effect on focus formation (Fig. 4C and D). This suggests that DNA uptake is dominated by eDNA that is produced within the biofilm either by lysis or by secretion through the type 4 secretion system. To assess this hypothesis, we incubated the colonies in the presence of DNase. Indeed, the density of foci was reduced by DNase treatment, but foci were still observed at a lower level (Fig. 4B, D). After 2 h, the density of foci was indistinguishable between the three conditions (Fig. 4E).

In conclusion, eDNA is most likely involved in forming ComE foci. However, ComE foci form even in the presence of nucleases (e.g. DNase). Therefore, ComE focus formation is not useful as an indicator for DNA uptake in gonococcal colonies.

2.4. Spatio-temporal dynamics of transformation

Finally, we investigated how efficiently colony-dwelling gonococci transformed with externally added DNA. To be able to detect transformation with spatial and temporal resolution, we generated a reporter strain containing the gene encoding for sfGFP. In strain *wt**, we inserted a point mutation in *sfgfp* to create a premature stop-codon in the chromophore region. Therefore, only truncated, non-fluorescent sfGFP is expressed (*$sfgfp_{nf}$*). When transformation replaces *$sfgfp_{nf}$* by native *sfgfp*, the transformed cell becomes fluorescent. Because *sfgfp* and *$sfgfp_{nf}$* differ only by a single nucleotide, the recombination probability should be high.

We added DNA to pre-formed gonococcal colonies and incubated for 4 h. We find that cells were transformed with 3 kb fragments within this time period (Fig. 5A). By contrast, no transformation events were observed for gonococcal DNA or 300 bp fragments. For 3 kb DNA, we counted the number of fluorescent cells per colony and found that this number increased between 1 h and 2 h after addition of eDNA (Fig. 5B). The time delay between addition of DNA and detection of fluorescence is most likely caused by the fact that transformed cells must produce sfGFP molecules before their fluorescence becomes detectable. Thereafter, both new transformation events and division of transformants increase the number of fluorescent cells per colony. The fact that the number of fluorescent cells per colony does not increase with time after 2 h indicates that no transformation occurs after 2 h or even earlier. To investigate the spatial distribution of transformants, we determined the number of fluorescent cells per volume as a function of penetration depth and time (Fig. 5C). At a penetration depth larger than 6 μm, no

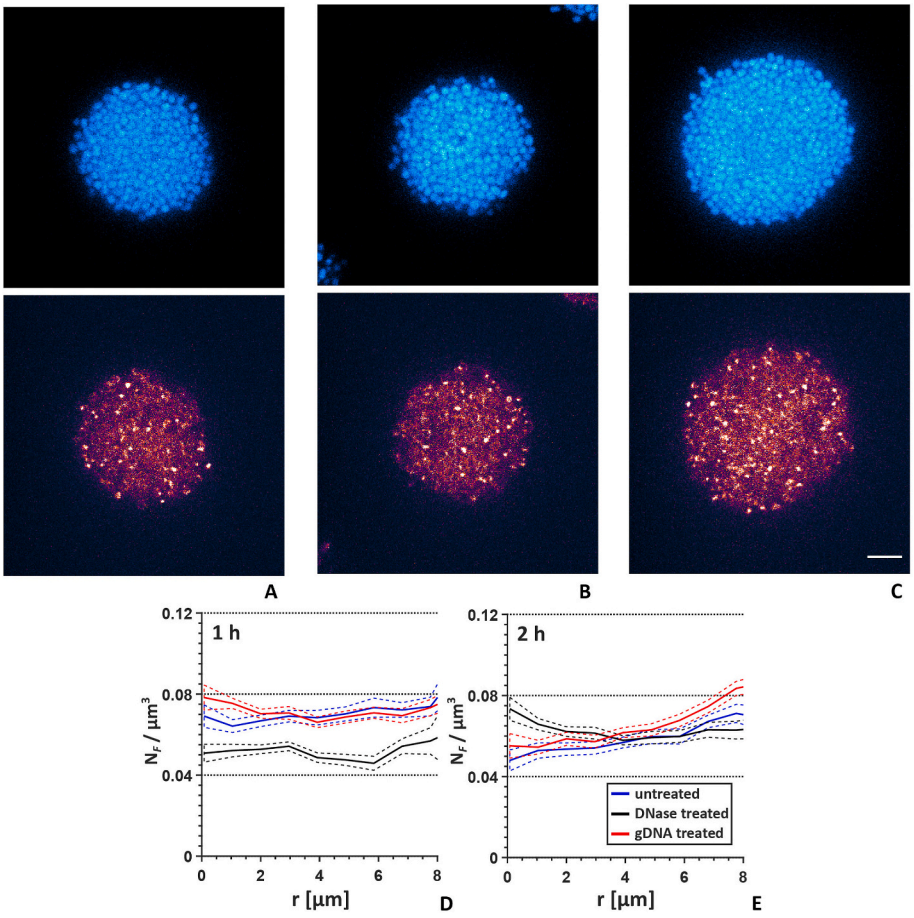

Fig. 4. Focal dynamics of the DNA uptake chaperone ComE. (A–C) Typical confocal slices of colonies formed by strain *comE-mcherry* (NG195) at t = 1 h. Upper images: GFP signal denoting cell positions. Lower images: ComE-mCherry. A) untreated, B) DNase treated, C) treated with gonococcal DNA. (D–E) Density (foci per µm^3) of ComE-mCherry foci within colonies as a function of the distance (r) to the colony contour at different time points without treatment (blue), with DNase (black), with gonococcal DNA (red). Dotted lines represent standard errors of 30 colonies. Data averaged with a sliding window of 1 µm. Scale bar: 5 µm. (For interpretation of the references to color in this figure legend, the reader is referred to the Web version of this article.)

transformants were detected, indicating that cells residing in the center of the colony are poorly transformable. Our previous experiments have shown that 3 kb fragments readily reach the center of the colony within 1 h (see Fig. 2); therefore, poor transformation in the colony core is not the result of a lack of transformable eDNA.

In conclusion, we find that transformation of 3 kb DUS + DNA fragments is limited to the periphery of colonies of freshly assembled colonies. Poor transformation of cells in the colony core is not the result of lacking eDNA, but most likely of reduced competence for transformation.

3. Discussion

3.1. Penetration and retention of external DNA depend on DNA length and DUS

We found that the penetration dynamics of (DUS-) DNA and its retention depend on the length of the nucleotide chain. Within 30 min, 300 bp DUS- DNA fragments distribute homogeneously within the colony and are retained at a low level. Larger DNA fragments form a concentration gradient whereby the concentration at the center of the colony is lowest, signifying hindered penetration into the colony. Penetration is slower, because DNA molecules whose length exceeds the Kuhn segment length of ~ 300 bp become entangled within the biofilm [11,42,43]. It is not clear, however, why more of the longer DNA fragments are retained within colonies. We propose the following explanation. eDNA is likely to be bound to the cells or the extracellular matrix (ECM). We expect that the integration of DNA into the ECM network is a slow process. Since long DNA molecules are more stationary than short DNA molecules, they are likely to be integrated in a more efficient way. DNA from *E. coli* contains several truncated DUS and, therefore, is likely to show low level binding to the minor pilin ComP, which is known to bind DNA in a DUS-specific fashion [18].

The DUS increased the amount of 300 bp and 3 kb DNA that was retained within the colonies. The retained fragments include eDNA and DNA taken up into the periplasm. Within 1 h, 3 kb fragments have penetrated the entire colony. Assuming a typical length of 1 kb for a single gene, the 3 kb fragment has the size of a typical operon, suggesting that DNA encoding for an entire operon is mobile enough to cover distances exceeding 10 µm. Interestingly, the amount of gonococcal DNA retained within the colony was considerably lower compared to the amount of *E. coli* gDNA. Very little gonococcal DNA reached the center of the colony. The central DNA is most likely dominated by the plasmid DNA contained within the DNA isolated from *N. gonorrhoeae*. We propose that this inefficient penetration and retention results from strong binding of gonococcal DNA to T4P and from DNA uptake, causing reduced diffusivity within the colony. Penetration and retention of DNA isolated from *N. cinerea* are even less efficient. This reduced efficiency might be explained by the different methylation pattern between both species. In agreement with this explanation, the nuclease Nuc has a stronger effect in *N. cinerea* DNA than on *N. gonorrhoeae* DNA. Moreover, the plasmids contained within the total DNA contents are likely to affect the pattern of DNA fluorescence. *N. cinerea* DNA preparations show discrete bands which suggest the presence of a plasmid with a higher molecular weight than the *N. gonorrhoeae* plasmid (Fig. S6).

We conclude that a combination of DNA length, unspecific binding, and specific binding governs DNA mobility within gonococcal colonies. Importantly, diffusivity of gonococcal DNA is restricted.

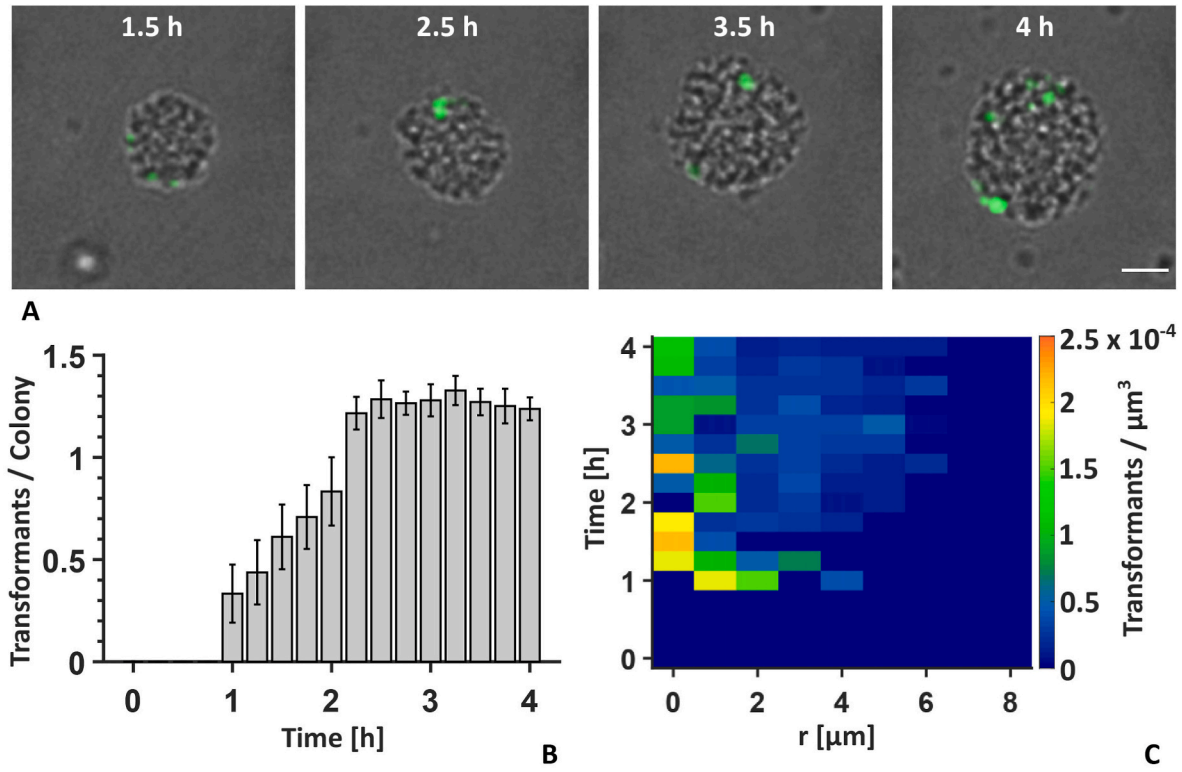

Fig. 5. Transformation in gonococcal colonies formed by strain *wt* sfgfp*$_{nf}$. 3 kb fragments containing DUS and a functional *sfgfp* sequence were added to colonies at t = 0. Transformants were identified by their fluorescence signal. A) Timelapse of single colony at indicated time points. Scale bar: 5 µm. B) Average number of transformants per colony with at least one transformation event. C) Transformants per colony volume as a function of the distance (r) to the colony contour in color code. (For interpretation of the references to color in this figure legend, the reader is referred to the Web version of this article.)

3.2. Within colonies ComE foci formation is caused by uptake of eDNA and other mechanisms

Previously, we have shown that ComE-mCherry forms foci at the site of DNA uptake in planktonic gonococci [22]. These foci form within minutes after addition of external DNA. Similarly, *V. cholerae* ComEA-mCherry forms foci [44], and therefore focus formation was used to detect DNA uptake in single cells [45]. Here, we intended to follow the same approach and detect DNA uptake in gonococcal colonies. However, the density profile of ComE-mCherry foci did not mirror the concentration profile of fluorescently labeled gonococcal DNA. While fluorescent DNA accumulated at the periphery, the profile of ComE-mCherry focus density was flat and indistinguishable from the profile of untreated colonies. These results indicate that DNA uptake is dominated by eDNA produced within the colonies. Even in young, 1 h old, colonies, a low fraction of cells are lysed [36]. Their neighboring bacteria are likely to take up their DNA. Furthermore, single stranded DNA is secreted through the type 4 secretion system [26] and can be taken up by surrounding cells. eDNA produced by lysis and secretion may saturate ComE [22] and inhibit uptake of externally added DNA.

Unexpectedly, ComE-mCherry focus formation was clearly detectable even during DNase treatment, indicating that foci form in the absence of eDNA. Recent studies highlight that bacteria can form tubular protrusions, called nanotubes, that bridge neighboring cells. These nanotube-bridges are subsequently used to shuttle cellular components, including DNA, between individual cells, while simultaneously bypassing the extracellular space [46]. Furthermore, gonococci are also known to create extracellular outer membrane vesicles, which could act as an alternate pathway for exchange of genetic material while avoiding the extracellular space [47,48]. Both mechanisms of DNA exchange would allow gonococci to maintain foci formation and uptake, in the presence of nucleases. Whether or not *N. gonorrhoeae* forms nanotubes remains to be shown, however. Finally, we cannot rule out that association with gonococci can protect from DNase cleavage or that ComE forms foci by a mechanism that is completely independent of DNA.

3.3. Transformation occurs preferentially at the periphery of freshly assembled colonies

We found transformation with 3 kb DUS+ DNA fragments, but with 300 bp DUS+ DNA fragments and gonococcal DNA, no transformation was observed. Most likely, the reason for this is that these short fragments have a very poor recombination rate [20]. For gonococcal DNA, we suggest that the DNA uptake machine [22] or the recombination machine may be saturated with DNA that transforms but does not repair the point mutation within *sfgfp*. Transformation of 3 kb DUS+ DNA was limited to the periphery of colonies, with very limited transformation in the inner layers of gonococcal cell aggregates. Taken together, gonococci transform only at the edge of young colonies. This observation agrees with previous reports, which highlight that gene transfer might be confined to the outer layers of bacterial aggregates and biofilms [49,50]. It has been proposed that this is likely caused by a large fraction of recipient cells not receiving transformable DNA due to gradients formed within the cell aggregate, which reduce availability of eDNA [51]. However, we showed that Cy3-labeled 3 kb fragments readily reach the inner core of colonies. Thus, we can exclude a lack of transformable DNA as a reason for limited transformation in the center of gonococcal colonies and conclude that low competence for transformation is the reason that transformants were hardly detected at the center of the colony. Previously, we showed that after 2 h, only cells at the periphery proliferate actively [36]. Possibly, the physiology of central cells does not support transformation.

Assuming a density of 0.3 cells/µm^3 and $2{\cdot}10^{-4}$ transformants/µm^3 at the edge of the colony, the fraction of transformants after 2 h to 4 h, is

$\approx 10^{-3}$. When averaged over the entire colony, the fraction is $< 10^{-4}$. In an earlier study, we investigated the rate of gene transfer between two gonococcal strains in colonies [38]. In that study, we probed the transfer of a gene encoding for a fluorescent protein adjacent to a gene encoding for antibiotic resistance. In the present study, we probed replacement of a single nucleotide by recombination which should occur at a much higher rate compared to the de novo acquisition of full genes [52]. Nevertheless, the fraction of transformants after 4 h to 5 h were comparable [38].

Taken together, we conclude that the rates of transformation in gonococcal colonies are low because transformation is localized to the periphery.

4. Conclusion

We show that the mobility of DNA within gonococcal colonies is governed by a complex interplay between DNA length, and binding by the DNA uptake sequence. DNA fragments long enough to contain multiple genes or an operon penetrate the colony within 1 h. Yet, despite the presence of nucleases within gonococcal colonies which are likely to reduce its length, DNA from gonococci is trapped. Furthermore, we show that transformation by external DNA fragments occurs only at the edge of colonies, suggesting that colony-dwelling bacteria rapidly switch off competence. In future studies, it will be interesting to find out whether stress conditions promote gene transfer within colonies.

5. Materials & methods

5.1. Growth media for N. gonorrhoeae

Gonococcal (GC) base agar was made from 10 g/l dehydrated agar (BD Biosciences), 5 g/l NaCl (Roth), 4 g/l K_2HPO_4 (Roth), 1 g/l KH_2PO_4 (Roth), 15 g/l Proteose Peptone No. 3 (BD Biosciences), 0.5 g/l soluble starch (Sigma-Aldrich) and supplemented with 1% IsoVitaleX (IVX). IVX was made from 1 g/l D-glucose (Roth), 0.1 g/l L-glutamine (Roth), 0.289 g/l L-cysteine-HCL x H_2O (Roth), 1 mg/l thiamine pyrophosphate (Sigma-Aldrich), 0.2 mg/l $Fe(NO_3)_3$ (Sigma-Aldrich), 0.03 mg/l thiamine HCL (Roth), 0.13 mg/l 4-aminobenzoic acid (Sigma-Aldrich), 2.5 mg/l β-nicotinamide adenine dinucleotide (Roth), and 0.1 mg/l vitamin B12 (Sigma-Aldrich). GC liquid medium is identical to the base agar composition but lacks both agar and starch.

5.2. Bacterial strains

All strains are *opa*- selected derivatives of *N. gonorrhoeae* MS11 with *ΔG4* (NG150) as parental strain. Wt gonococci undergo pilin antigenic variation at a high frequency [53]. This can lead to reduction of piliation or loss of piliation. Since T4P govern cell-to-cell attraction in gonococcal colonies [7,54], pilin antigenic variation would potentially influence the results of this study. Therefore, we deleted the G4 motive required for pilin antigenic variation in all strains [55]. *wt** (NG194) has a gene encoding for a sfGFP integrated in an intergenic region. GFP fluorescence is used to detect the positions of individual cells within the colony.

A *nuc*-deficient variant of strain *wt** (NG194) was created by transforming genomic DNA of strain *GV1 Δnuc* (NG058) [20] into cells of *wt**. Transformants were selected on GC-plates containing kanamycin, yielding the final strain NG235 (*Δnuc*). Correct insertion of the kanamycin cassette into *nuc* was verified by PCR with primers NB084 and NB085.

We generated a strain for detecting transformation with eDNA. In particular, *wt* sfgfp$_{nf}$* (NG233) was designed to be non-fluorescent due to a single nucleotide substitution that creates a premature stop codon within the *sfgfp* gene. Recombination with the functional copy of *sfgfp* creates fluorescent gonococci. Therefore, fluorescent bacteria signify transformation. The transformation reporter strain (*wt* sfgfp$_{nf}$*) was generated by introducing a point mutation into the chromophore region of *sfgfp* of strain *wt** (NG194) [36]. To this end, we subcloned *sfgfp* into vector pLAS and introduced the point mutation at position 201 of the *sfgfp* coding sequence by site-directed mutagenesis using back-to-back primers NB073 and NB074. The resulting plasmid was then transformed into strain *mcherry* (NG232). Clones were selected on plates containing erythromycin and subsequently sequenced to confirm the integration of the point mutation, yielding the final strain *wt* sfgfp$_{nf}$* (NG233).

Strain *comE-mcherry* was generated by, first, transforming genomic DNA of strain *comE-mcherry ΔpilV* (NG068) [22] into strain *ΔG4* (NG150) [32], thereby transferring the *comE-mcherry* insert into the *ΔG4* background. Transformants were selected on plates containing kanamycin. A positive clone of this transformation step was subsequently transformed with genomic DNA of strain *gfp* (NG151) [32] and transformants were selected on GC-agar plates containing erythromycin; thereby, yielding the final strain *comE-mcherry* (NG195).

Strain *mcherry* was created by amplifying *PpilE-mcherry* from genomic DNA of strain *N400 mcherry* (NG065) [41] with primers NB069 and NB070. The product was integrated into vector pIGA after XhoI and KpnI restriction digest. The resulting plasmid was subsequently transformed into strain *ΔG4* (NG150) [32], yielding the final strain *mcherry* (NG232).

5.3. Confocal microscopy setup

All microscopy data was acquired with a Ti-E inverted microscope (Nikon) equipped with a CSU-X1 (Yokogawa) spinning disk unit and a 100x, 1.49 NA CFI Apo Tirf oil immersion objective (Nikon). Image acquisition was done with an EMCCD camera (iXon 897, Andor) with an image size of 512 x 512 pixels, and a pixel width of 0.079 μm. Fluorophores were excited with 488 nm and 561 nm wavelengths. Exposure times were set to 50 ms.

5.4. Preparation of DNA samples and fluorescent labelling with Cy3

In order to obtain DNA of *N. gonorrhoeae*, bacteria of strain *ΔG4* (NG150) were plated on GC-agar plates and subsequently incubated overnight at 37 °C with 5% CO_2. Cells were resuspended in PBS (Gibco/Life Technologies) and pelleted by brief centrifugation. Finally, DNA was obtained using the DNeasy Blood & Tissue Kit (Qiagen) according to the instructions provided by the manual of the kit. DNA of *N. cinerea* (DSM No: 4630, ATCC 14685, NCTC 10294) was obtained by the same procedure. For genomic DNA of *E. coli*, cells of strain *DH5α* were grown overnight in a 5 ml liquid culture of LB-broth (Carl Roth) at 37 °C. Again, cells were pelleted by centrifugation and the DNA was isolated with the DNeasy Blood & Tissue Kit. We characterized the length distributions of isolated genomic DNA (Fig. S6) and found that genomic DNA isolated from *N. gonorrhoeae* showed multiple discrete bands of several kbp length. These bands most likely indicate the presence of (supercoiled and nicked) plasmid DNA [56]. To further characterize this putative plasmid DNA, we purified *ΔG4* (NG150) genomic DNA with the QIAquick PCR Purification Kit (Qiagen), which depletes fragments exceeding a length scale of ~10 kbp and, thus, enriches the plasmid DNA in the sample (Fig. S6). Using the primer pair NB092 and NB093, we verified that the MS11 plasmid with the accession number CP003910 (cryptic plasmid [56]) was present. We conclude that gonococcal DNA consists of a mixture between fragments of chromosomal DNA and plasmid DNA.

3 kbp and 300 bp fragments were generated by PCR. Primer NB077 was used as a forward primer for fragments containing a DNA uptake sequence (DUS), with primer NB078 and NB079 acting as the reverse primer for 300 bp and 3 kbp fragments, respectively. For fragments lacking DUS, primer NB080 was used as the forward primer; with NB081 and NB082 as reverse primers for 300 bp and 3 kbp fragments. Genomic DNA of strain *ΔG4* (NG150) was used as template DNA.

In order to covalently attach Cy3 molecules to the nucleotide samples, we used the Label IT Nucleic Acid Labelling Kit, Cy3 (MIR3600, Mirus Bio LLC). All steps were performed according to the instructions lined out in the manual of the kit; however, we extended the incubation time of the labelling reaction to 2 h to ensure proper labelling of the DNA samples. To ensure sufficient yield of Cy3-sample DNA, we pooled multiple labeling reactions before the experiments were started. To correct of differences in labeling efficiency, we used a fluorescence spectrometer to measure the fluorescence intensity of all labeled DNA samples at a wavelength of 562 nm and normalized the fluorescence intensity of the confocal images to these values.

5.5. Confocal imaging of Cy3-DNA in gonococcal colonies

Cells of strain *wt** (NG194) and *Δnuc* (NG235) were grown on GC-agar plates at 37 °C, 5% CO_2 overnight, subsequently scraped and resuspended in sterile filtered liquid GC medium which was supplemented with 7 mM $MgCl_2$ and warmed to 37 °C. The optical density (OD_{600}) was adjusted to 0.1 and 500 μl of the suspension were incubated in a shaking-incubator (250 rpm, 37 °C, 5% CO_2) for 30 min. Afterwards, 200 μl were added into a poly-L-lysine coated μ-Slide 8 Well (Cat.No. 80824, Ibidi) and the plate was incubated for another 30 min (w/o shaking). Finally, a 100 μl sample of GC-medium containing 1.5 μg of fluorescently labeled Cy-3 DNA was added and the well plate was transferred to the microscope.

During image acquisition, we imaged random colonies throughout a period of 2 h. For each colony, we obtained a z-stack of 27 images, with a z-spacing of 0.2 μm per image, close to the equatorial, lateral plane of the colony; resulting in a 3D data set that accounts for a total height of 5 μm within the colony. Laser powers were set to 50% and 5% (of 100 mW) for 561 nm (Cy3-DNA) and 488 nm (sfGFP, denoting cell positions) lasers, respectively.

5.6. Determination of radial fluorescence intensity profiles of Cy3-DNA

The radial intensity profiles of fluorescently labeled DNA within colonies were determined and analyzed with proprietary Matlab (MathWorks) scripts. Data obtained from different colonies was averaged starting at the colony periphery. Since eDNA enters the colony at the surface, the position with respect to the edge of the colony is relevant. The colony size is variable and, therefore, the number of data points contributing to the fluorescence intensity at the center of the colony is variable accounting for the increased standard error in the data at the colony center.

Colony and cell detection were based on the identification of sfGFP fluorescence in each recording. We extracted the center of mass position (COM) of the colony and its radius (r) from confocal microscopy data sets by creating a single averaged image of the 3D image stack from which we subtracted a Gaussian-blurred duplicate (blur radius 10 px, roughly equal to the cell diameter). Colonies were then detected by applying the Matlab function *imfindcircles* (radius range 100 – 300 pixels for colonies with typical radius 15 μ m).

Next, detection of Cy3-DNA fluorescence intensities in the colonies was performed by first normalizing raw data intensities for different DNA samples. To this end, we scaled the pixel values of each image according to the fluorescence intensities we measured for different Cy3-DNA samples. The normalized images were subsequently averaged (over 5 μm) in z-direction. We then performed a background subtraction by removing the intensity of the regions beyond the colony from the image. Background intensity profiles were obtained by fitting a second degree 2D polynomial $p_0 + p_{10}x + p_{01}y + p_{11}xy + p_{20}x^2 + p_{02}y^2$ with coefficients p_{ij} to an image where the colony has been removed (setting the corresponding pixel values to NaN). The final pixel-wise fluorescence intensities were then distributed into radial bins to obtain the radial fluorescence intensity profiles in the colonies with respect to their distance to the colony contour.

5.7. Confocal imaging of ComE foci within gonococcal colonies

Cells of strain *comE-mcherry* (NG195) were grown on GC-agar plates at 37 °C, 5% CO_2 overnight, subsequently scraped and resuspended in sterile filtered liquid GC medium which was supplemented with 7 mM $MgCl_2$ and warmed to 37 °C. The optical density (OD_{600}) of the solution was adjusted to 0.1 in a volume of 500 μl. Next, either 10 units of DNaseI (New England Biolabs) or 1.5 μg DNA of *N. gonorrhoeae* strain *ΔG4* (NG150) were added to the suspension. For untreated controls, an equal amount of medium was added instead. Subsequently, the mix was shaken for 30 min at 37 °C, 5% CO_2 in an incubator at 250 rpm. Finally, 200 μl were added into a poly-L-lysine coated μ-Slide 8 Well (Cat.No. 80824, Ibidi) and imaging of colonies was started immediately.

Random colonies were imaged after 0, 1 and 2 h. Again, for every colony imaged, we acquired a z-stack of 27 images, with a z-spacing of 0.2 μm per image, close to the equatorial, lateral plane of the colony; thus, obtaining a 3D data set that resembles a total height of 5 μm within the colony. Laser powers were set to 15% and 5% for 561 nm (ComE-mCherry) and 488 nm (GFP, denoting cell positions) lasers, respectively.

5.8. Determination of radial ComE focal density profiles

Determination of ComE focal densities within gonococcal colonies required both the detection of ComE foci and the colony itself. Colony detection was based on the same Matlab routines described earlier (see paragraph for Cy3-DNA detection). ComE foci (Fig. S5) were detected as follows. First, we averaged the 3D image stacks over 5 μm along the z-direction. From this average, we created a median-smoothed duplicate using the *immedfiltt2* Matlab function (smoothing window 20 x 20 pixels). The smoothed copy was subtracted from the initial image, which eliminated any background noise and left only the intensity peaks of the foci. Peak detection was performed with the *pkfnd* and *cntrd* functions of the IDL-tracking suite (from The Matlab Particle Tracking Repository by Daniel Blair and Eric Dufresne [57]) for which we chose a blob diameter of 10 pixel corresponding to roughly one cell diameter. The intensity threshold was adjusted separately for each timepoint, as we found that the fluorescence intensity of ComE-mCherry decreased considerably over the course of the experiment. More specifically, the threshold was chosen as the Gauss radius of the noise intensity distribution extracted from the histogram of the intensity of the image. The detected foci positions were then distributed into radial bins to obtain the DNA foci density with respect to the distance to the colony contour. In this experiment, we were interested in the intensity profile and in the comparison between different conditions at a specific time point. Therefore, the fact that the density of detected foci might vary as a function of time due to reduced mCherry fluorescence is not relevant here.

5.9. Confocal imaging of transformation events with spatial and temporal resolution

Cells of strain *wt** *sfgfp$_{nf}$* (NG233) were grown on GC-agar plates overnight at 37 °C and 5% CO_2. Cells were resuspended in sterile filtered GC medium supplemented with 7 mM $MgCl_2$ and the optical density was adjusted to 0.1. 500 μl of the cell suspension were inoculated into a fresh tube, which was then incubated for another 30 min under shaking conditions (250 rpm, 37 °C, 5% CO_2). Thereafter, 200 μl were transferred to a poly-L-lysine coated μ-Slide 8 Well (Cat.No. 80824, Ibidi). The well plate was subsequently incubated for another 30 min to allow colonies to form. Afterwards, 100 μl GC-medium containing 1.5 μg of DNA was added to the well and imaging of gonococcal colonies was started immediately.

The added gonococcal DNA was derived from strain *wt** (NG194). 3 kb and 300 bp fragments were created by PCR using primer pair NB090 (2) and NB091 for 300 bp fragments, and primer pair NB088 and NB089 for 3 kb fragments. In both cases, the primers added a single DNA uptake sequence (DUS) to the fragment. Genomic DNA of strain wt* was used as

a template, to ensure that the fragments contained the native *sfgfp* chromophore sequence.

Image acquisition was done in a multipoint recording: we designated four areas within the well plate to be imaged over a period of 4 h. To increase the overall area, we can cover during imaging, we applied tiling of 5x5 images. Each area was imaged and recorded every 15 min. For each imaging step, we obtained a 5 μm stack approx. 10 μm above the surface of the well plate, with each stack comprising of 27 images with a z-spacing of 0.2 μm; yielding a 3D data set of multiple colonies per time point. Transformed cells were visualized with a 488 nm laser set to 5% as denoted by sfGFP expression. To extract the contours of colonies, we also acquired a brightfield image for every z-stack.

5.10. Determination of radial transformant densities

The detection of transformed cells within gonococcal colonies with spatial and temporal resolution was performed as follows. First, we extracted radii (r) and center of mass positions (COM) for all colonies in each brightfield image. To this end, images were smoothed with a Gaussian blur filter (sigma = 2 px) to remove salt and pepper noise. We analyzed the local intensity variance (over a 15 x 15 px window) to determine the edge of the colonies. The local intensity variance within the colony was higher compared to the background. Variance images were thresholded which resulted in a binary representation of the field of view [7]. Using binary erosion and dilation operations, a filled and corrected colony mask was obtained, from which we determined the colony extent (r) and the x, y-coordinates of the COM. The z-position of the colony COM was calculated by multiplying the radius (r) with a factor of 0.85 [31].

To detect transformed cells in the fluorescence images, we created a binary mask with 7x the standard deviation of the image intensity as the threshold value. The Matlab function *regionprops* was used to obtain x-, y- and z-positions for every fluorescent spot in each image. We then combined all spots within a range of 2.4 μm in z-orientation into a single spot. We found this procedure to be an appropriate solution to obtain the true number of transformed cells in z-direction. Similarly, we combined spots if they were in a range of 4 μm in x- and y-direction to account for multiple transformants in close proximity to one another. This was done in order to avoid the detection of cell division events as opposed to transformation events.

Next, detected transformants needed to be linked to their respective colony so that we can determine the transformation density. To this end, we calculated the distance to all colony COMs in the brightfield image in x and y direction and picked the colony for which this distance is smallest. From here, we determined the transformant density by dividing the number of spots in a certain spherical shell of the colony by the area of this shell.

Author contributions

NB, MH, and BM designed research. NB performed research. MH and NB analysed data. NB and BM wrote the manuscript. Given her role as Editor, Berenike Maier had no involvement in the peer review of this article and has no access to information regarding its peer review. Full responsibility for the editorial process for this article was delegated to Ákos T. Kovács.

Declaration of competing interest

The authors declare that they have no known competing financial interests or personal relationships that could have appeared to influence the work reported in this paper.

Acknowledgements

We thank Gabriele Schneider for support with strain construction, Magdalene So for supplying us with *N. cinerea*, and the Maier lab for stimulating discussions. This work has been funded by the Deutsche Forschungsgemeinschaft through grant MA3898, the IHRS BioSoft, and the Center for Molecular Medicine Cologne.

Appendix A. Supplementary data

Supplementary data to this article can be found online at https://doi.org/10.1016/j.bioflm.2022.100078.

References

[1] Abe K, Nomura N, Suzuki S. Biofilms: hot spots of horizontal gene transfer (HGT) in aquatic environments, with a focus on a new HGT mechanism. FEMS Microbiol Ecol 2020;96(5).
[2] Uruen C, Chopo-Escuin G, Tommassen J, Mainar-Jaime RC, Arenas J. Biofilms as promoters of bacterial antibiotic resistance and tolerance. Antibiotics-Basel 2021;10(1).
[3] Roder HL, et al. Biofilms can act as plasmid reserves in the absence of plasmid specific selection. Npj Biofilms Microbi 2021;7(1).
[4] van Gestel J, et al. Short-range quorum sensing controls horizontal gene transfer at micron scale in bacterial communities. Nat Commun 2021;12(1).
[5] Maier B. How physical interactions shape bacterial biofilms. Annu Rev Biophys 2021;50:401–17.
[6] Hallatschek O, Hersen P, Ramanathan S, Nelson DR. Genetic drift at expanding frontiers promotes gene segregation. P Natl Acad Sci USA 2007;104(50):19926–30.
[7] Oldewurtel ER, Kouzel N, Dewenter L, Henseler K, Maier B. Differential interaction forces govern bacterial sorting in early biofilms. Elife 2015;4.
[8] Zollner R, et al. Type IV pilin post-translational modifications modulate material properties of bacterial colonies. Biophys J 2019;116(5):938–47.
[9] Zhang ZS, Nadezhina E, Wilkinson KJ. Quantifying diffusion in a biofilm of Streptococcus mutans. Antimicrob Agents Chemother 2011;55(3):1075–81.
[10] Stewart PS. Diffusion in biofilms. J Bacteriol 2003;185(5):1485–91.
[11] Sankaran J, et al. Single microcolony diffusion analysis in Pseudomonas aeruginosa biofilms. NPJ Biofilms Microbiomes 2019;5(1):35.
[12] Dubnau D, Blokesch M. Mechanisms of DNA uptake by naturally competent bacteria. Annu Rev Genet 2019;53:217–37.
[13] Craig L, Forest KT, Maier B. Type IV pili: dynamics, biophysics and functional consequences. Nat Rev Microbiol 2019;17(7):429–40.
[14] Aas FE, et al. Competence for natural transformation in Neisseria gonorrhoeae: components of DNA binding and uptake linked to type IV pilus expression. Mol Microbiol 2002;46(3):749–60.
[15] Aas FE, Lovold C, Koomey M. An inhibitor of DNA binding and uptake events dictates the proficiency of genetic transformation in Neisseria gonorrhoeae: mechanism of action and links to Type IV pilus expression. Mol Microbiol 2002;46(5):1441–50.
[16] Goodman SD, Scocca JJ. Identification and arrangement of the DNA-sequence recognized in specific transformation of neisseria-gonorrhoeae. P Natl Acad Sci USA 1988;85(18):6982–6.
[17] Frye SA, Nilsen M, Tonjum T, Ambur H. Dialects of the DNA uptake sequence in neisseriaceae. PLoS Genet 2013;9(4).
[18] Cehovin A, et al. Specific DNA recognition mediated by a type IV pilin. P Natl Acad Sci USA 2013;110(8):3065–70.
[19] Berry JL, Cehovin A, McDowell MA, Lea SM, Pelicic V. Functional analysis of the interdependence between DNA uptake sequence and its cognate ComP receptor during natural transformation in Neisseria species. PLoS Genet 2013;9(12).
[20] Hepp C, Gangel H, Henseler K, Gunther N, Maier B. Single-stranded DNA uptake during gonococcal transformation. J Bacteriol 2016;198(18):2515–23.
[21] Hepp C, Maier B. Kinetics of DNA uptake during transformation provide evidence for a translocation ratchet mechanism. P Natl Acad Sci USA 2016;113(44):12467–72.
[22] Gangel H, et al. Concerted spatio-temporal dynamics of imported DNA and ComE DNA uptake protein during gonococcal transformation. PLoS Pathog 2014;10(4).
[23] Steichen CT, Shao JQ, Ketterer MR, Apicella MA. Gonococcal cervicitis: a role for biofilm in pathogenesis. J Infect Dis 2008;198(12):1856–61.
[24] Falsetta ML, et al. The composition and metabolic phenotype of Neisseria gonorrhoeae biofilms. Front Microbiol 2011;2:75.
[25] Steichen CT, Cho C, Shao JQ, Apicella MA. The Neisseria gonorrhoeae biofilm matrix contains DNA, and an endogenous nuclease controls its incorporation. Infect Immun 2011;79(4):1504–11.
[26] Zweig M, et al. Secreted single-stranded DNA is involved in the initial phase of biofilm formation by Neisseria gonorrhoeae. Environ Microbiol 2014;16(4):1040–52.
[27] Dewenter L, Volkmann TE, Maier B. Oxygen governs gonococcal microcolony stability by enhancing the interaction force between type IV pili. Integr Biol-Uk 2015;7(10):1161–70.
[28] Merz AJ, So M, Sheetz MP. Pilus retraction powers bacterial twitching motility. Nature 2000;407(6800):98–102.
[29] Kraus-Römer S, Wielert I, Rathmann I, Grossbach J, Maier B. External stresses affect gonococcal type 4 pilus dynamics. Front Microbiol 2022;13:839711.
[30] Holz C, Opitz D, Mehlich J, Ravoo BJ, Maier B. Bacterial motility and clustering guided by microcontact printing. Nano Lett 2009;9(12):4553–7.

[31] Higashi DL, et al. Dynamics of Neisseria gonorrhoeae attachment: microcolony development, cortical plaque formation, and cytoprotection. Infect Immun 2007;75(10):4743–53.
[32] Welker A, et al. Molecular motors govern liquidlike ordering and fusion dynamics of bacterial colonies. Phys Rev Lett 2018;121(11).
[33] Bonazzi D, et al. Intermittent pili-mediated forces fluidize Neisseria meningitidis aggregates promoting vascular colonization. Cell 2018;174(1):143–+.
[34] Ponisch W, Weber CA, Juckeland G, Biais N, Zaburdaev V. Multiscale modeling of bacterial colonies: how pili mediate the dynamics of single cells and cellular aggregates. New J Phys 2017;19.
[35] Hennes M, Cronenberg T, Maier B. Caging dynamics in bacterial colonies. Phys. Rev. Res. 2022;4:013187.
[36] Welker A, et al. Spatiotemporal dynamics of growth and death within spherical bacterial colonies. Biophys J 2021;120(16):3418–28.
[37] Ponisch W, et al. Pili mediated intercellular forces shape heterogeneous bacterial microcolonies prior to multicellular differentiation. Sci Rep 2018;8(1):16567.
[38] Kouzel N, Oldewurtel ER, Maier B. Gene transfer efficiency in gonococcal biofilms: role of biofilm age, architecture, and pilin antigenic variation. J Bacteriol 2015;197(14):2422–31.
[39] Juneau RA, Stevens JS, Apicella MA, Criss AK. A thermonuclease of Neisseria gonorrhoeae enhances bacterial escape from killing by neutrophil extracellular traps. J Infect Dis 2015;212(2):316–24.
[40] Roberts RJ, Vincze T, Posfai J, Macelis D. REBASE-a database for DNA restriction and modification: enzymes, genes and genomes. Nucleic Acids Res 2015;43(D1):D298–9.
[41] Kim WJ, et al. Commensal Neisseria kill Neisseria gonorrhoeae through a DNA-dependent mechanism. Cell Host Microbe 2019;26(2):228–+.
[42] Yeon WC, Kannan B, Wohland T, Ng V. Colloidal crystals from surface-tension-assisted self-assembly: a novel matrix for single-molecule experiments. Langmuir 2008;24(21):12142–9.
[43] Doi M, Edwards SF. The theory of polymer dynamics. Oxford Science Publications; 1986.
[44] Seitz P, et al. ComEA is essential for the transfer of external DNA into the periplasm in naturally transformable Vibrio cholerae cells. PLoS Genet 2014;10(1).
[45] Borgeaud S, Metzger LC, Scrignari T, Blokesch M. The type VI secretion system of Vibrio cholerae fosters horizontal gene transfer. Science 2015;347(6217):63–7.
[46] Dubey GP, Ben-Yehuda S. Intercellular nanotubes mediate bacterial communication. Cell 2011;144(4):590–600.
[47] Ficht TA. Bacterial exchange via nanotubes: lessons learned from the history of molecular biology. Front Microbiol 2011;2.
[48] Deo P, et al. Outer membrane vesicles from Neisseria gonorrhoeae target PorB to mitochondria and induce apoptosis. PLoS Pathog 2018;14(3).
[49] Haagensen JAJ, Hansen SK, Johansen T, Molin S. In situ detection of horizontal transfer of mobile genetic elements. FEMS Microbiol Ecol 2002;42(2):261–8.
[50] Stalder T, Top E. Plasmid transfer in biofilms: a perspective on limitations and opportunities. Npj Biofilms Microbi 2016;2.
[51] Molin S, Tolker-Nielsen T. Gene transfer occurs with enhanced efficiency in biofilms and induces enhanced stabilisation of the biofilm structure. Curr Opin Biotechnol 2003;14(3):255–61.
[52] Power JJ, et al. Adaptive evolution of hybrid bacteria by horizontal gene transfer. P Natl Acad Sci USA 2021;118(10).
[53] Rotman E, Seifert HS. The genetics of Neisseria species. Annu Rev Genet 2014;48:405–31.
[54] Zollner R, Oldewurtel ER, Kouzel N, Maier B. Phase and antigenic variation govern competition dynamics through positioning in bacterial colonies. Sci Rep-Uk 2017;7.
[55] Cahoon LA, Seifert HS. An alternative DNA structure is necessary for pilin antigenic variation in Neisseria gonorrhoeae. Science 2009;325(5941):764–7.
[56] Cehovin A, Jolley KA, Maiden MCJ, Harrison OB, Tang CM. Association of Neisseria gonorrhoeae plasmids with distinct lineages and the economic status of their country of origin. J Infect Dis 2020;222(11):1826–36.
[57] Crocker JC, Grier DG. Methods of digital video microscopy for colloidal studies. J Colloid Interface Sci 1996;179:298.